Role of Conformational Dynamics in Sequence-Specific Autoantibody•ssDNA Recognition

Melissa J. Bobeck,[1] Gary D. Glick[1,2]

[1] *Department of Chemistry, University of Michigan, Ann Arbor, MI 48109-1055*

[2] *Department of Biological Chemistry, University of Michigan, Ann Arbor, MI 48109-1055*

Received 6 January 2007 ; accepted 22 January 2007
Published online 24 January 2007 in Wiley InterScience (www.interscience.wiley.com). DOI 10.1002/bip.20692

ABSTRACT:

11F8 is a sequence-specific monoclonal anti-ssDNA autoantibody isolated from a lupus prone mouse that forms pathogenic complexes with ssDNA, resulting in kidney damage. Prior studies show that specificity is mediated by a somatic mutation from serine at $^{31}V_H$ to arginine. Reversion back to serine in 11F8 resulted in >30-fold decrease in affinity and altered thermodynamic and kinetic parameters for sequence-specific recognition of its cognate ssDNA ligand. Mutagenesis and structural studies suggest that $^{R31}V_H$ contacts ssDNA via a salt bridge and a bidentate hydrogen bond and may further contribute to specificity by altering binding-site conformation. Fluorescence resonance energy transfer experiments were conducted to assess the kinetics of conformational change during 11F8•ssDNA association. The extent of rearrangement between the six complementary determining regions in the 11F8•ssDNA complex with germline serine or somatically mutated arginine at residue 31 of the heavy chain was examined. Our studies show that greater conformational change occurs in five of six complementarity determining regions after the heavy chain germline J558 sequence undergoes mutation to arginine at $^{31}V_H$. © 2007 Wiley Periodicals, Inc. Biopolymers 85: 481–489, 2007.

Keywords: binding induced conformational change; antibody dynamics; sequence-specific recognition of ssDNA; fluorescence resonance energy transfer; stopped-flow kinetics

This article was originally published online as an accepted preprint. The "Published Online" date corresponds to the preprint version. You can request a copy of the preprint by emailing the Biopolymers editorial office at biopolymers@wiley.com

Correspondence to: Gary D. Glick; e-mail: gglick@umich.edu
Contract grant sponsor: NIH
Contract grant number: GM 46831

INTRODUCTION

The vertebrate immune system contains sufficient diversification elements to recognize a vast array of antigens with high affinity and specificity. As such, antibody•antigen complexes are valuable model systems to study molecular recognition.[1,2] Conformational changes upon binding can be intimately linked to function, and extensive studies have been completed to try to understand both the structural and dynamic components of antibody•antigen recognition.[3,4] High-resolution structures of free antibody fragments, free antigens, and their complexes are known for some interactions, permitting a full characterization of the contacts and conformational adaptations involved in complex formation.[5–11] Recent studies have utilized techniques such as cryo-electron tomography, atomic force microscopy, and fluorescence resonance energy transfer to describe the time course of conformational rearrangement during binding.[12–14]

Antibodies that bind DNA (anti-DNA) are a hallmark of the autoimmune disease systemic lupus erythematosus (SLE). A subset of anti-DNA form complexes localized to the glomerular basement membrane of the kidney where thy can

illicit nephritis, which is responsible for the morbidity and mortality associated with lupus.[15,16] In previous studies, we generated a panel of anti-ssDNA monoclonal antibodies (mAbs) from a lupus prone mouse in attempts to differentiate pathogenic and benign anti-DNA.[17] Only one mAb in our panel, 11F8, induces nephritis when administered to healthy mice.[18] Binding site selection experiments for 11F8 reveal preference for a single high affinity consensus ssDNA, **1**, whose sequence and secondary structure are related to DNA antigens eluted from kidney tissue of SLE patients (Figure 1).[19–24] Selection experiments for clonally related nonpathogenic mAbs 9F11 and 15B10 revealed that these mAbs are not sequence-specific, and only display a preference for thymine-rich sequences.[25] Interestingly, the primary sequence of 11F8 differs from 9F11 and 15B10 by less than five amino acids localized in the variable region of the heavy chain.[28]

Somatic mutation from serine to arginine at residue 31 of the variable heavy chain ($^{31}V_H$) is the primary mediator of 11F8 sequence-specificity.[29] Mutagenesis experiments suggest a salt bridge and hydrogen bond interaction, and our data-driven model reveals a bidentate hydrogen bond between $^{R31}V_H$ with ^{C9}**1** that likely contributes to specificity.[26,30] Modeling experiments suggested that while the two ligated states (11F8•**1** and ^{R31S}11F8•**1**) are related in structure, the 11F8 interface consists of additional residues when arginine is at $^{31}V_H$ as compared to serine.[30] Further, the per residue backbone root mean square deviations for the light chain complementarity determining regions (LCDRs) (1.6 ± 0.3 Å), heavy chain complementrity regions (HCDRs) (1.8 ± 0.4 Å), and ssDNA (5.1 ± 2.2 Å) were slightly larger albeit still within error for the 11F8•**1** complexes with respect to the ^{R31S}11F8•**1** complexes (1.5 ± 0.3 Å, 1.6 ± 0.5 Å, and 3.6 ± 1.2 Å, respectively), suggesting that somatic mutation to arginine may afford greater binding-site flexibility during recognition.

Here we report a method based on the distance-dependent technique of fluorescence resonance energy transfer (FRET) in conjunction with stopped-flow measurements, to directly assess the kinetics and relative amplitudes of binding site conformational changes during mAb•ssDNA association. FRET amplitudes during association for complexes formed between fluorescein labeled 11F8 and tetramethylrhodamine labeled **1** are larger with arginine at $^{31}V_H$ with respect to serine. Thus, our ^{R31S}11F8•**1** system likely illustrates how the conserved ssDNA recognition hot spot ($^{Y32}V_L$, a hydrogen bonding side chain at $^{91}V_L$, and an aromatic at the tip of HCDR3) predisposes mAbs for thymine recognition, affording thymine intercalation at the binding site with minimal conformational change.[31] We hypothesize that following somatic mutation to arginine at $^{31}V_H$, greater conformational change during 11F8•**1** association affords additional protein•ssDNA contacts that result in sequence-specificity.

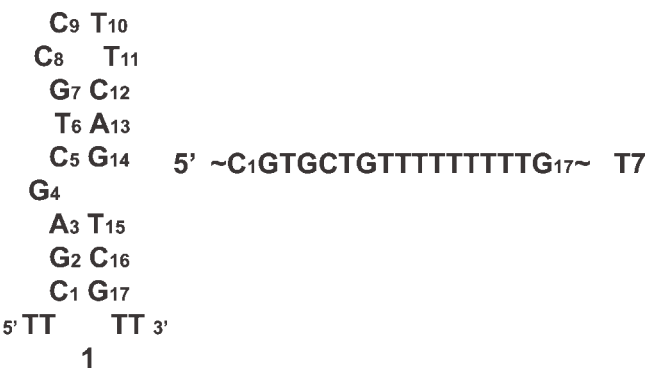

FIGURE 1 DNA ligands used in binding studies. Binding site selection experiments were conducted with 11F8 and 55-nucleotide long ssDNA constructs possessing a seven nucleotide-long random insert.[25] DNA of known sequence designed to prevent formation of stable secondary structure flanked the random region. Mutations produced during PCR amplification at multiple sites within the constant region afforded a stable secondary structure that was selected for by 11F8. **1** is the consensus sequence obtained from these experiments.[25] Additional nucleotides that initially flanked the stem-loop were PCR primers used in the selection experiments and were removed for these studies. Affinity and rate experiments were completed with 21-mer hairpin sequences as shown. Truncation does not increase affinity or alter binding properties.[26,27] In **T7**, positions 3, 8–14, and 16 of **1** are replaced with T.

MATERIALS AND METHODS

11F8 Cysteine Variant Expression, Purification, and Labeling

A his-tagged single chain 11F8 construct cloned into pET-28b(+) (Novagen, Madison WI) was used as the template for mutagenesis.[29] Plasmids encoding $^{T30C}V_H$, $^{S53C}V_H$, $^{Q105C}V_H$, $^{S10C}V_L$, $^{S60C}V_L$, $^{T94C}V_L$ and double mutants containing $^{R31S}V_H$ and each of the aforementioned six variants of 11F8 were constructed using site-directed mutagenesis according to the Quickchange protocol (Stratagene, La Jolla, CA). Successful incorporation of each mutation was confirmed by DNA sequencing. Large-scale expression and purification were performed as described for the wild-type protein with minor modification.[29] Briefly, denatured 11F8 variants were isolated from the insoluble bacteria pellet and purified with Ni^{2+} agarose (Qiagen, Santa Clarita, CA). Fractions containing protein were refolded by rapid dilution (1:200) into DNA binding buffer (50 m*M* $NaHPO_4$, pH 8, 150 m*M* NaCl, 0.1 m*M* TCEP (Tris (2-carboxyethyl) phosphine, hydrochloride)), containing oxidized glutathione (0.4 m*M*), reduced glutathione (4 m*M*), and 1% v/v single-stranded DNA agarose matrix with stirring for >24 h at 4°C.[32] The solution was poured through a fritted glass column to isolate protein bound resin. Resin was washed with five column volumes of DNA binding buffer containing 400 m*M* NaCl. Folded protein was eluted from the ssDNA column with DNA binding buffer containing NaCl (2*M*)

and urea (2*M*) and immediately exchanged into conjugation buffer (50 m*M* $NaHPO_4$, 150 m*M* NaCl, 0.1 m*M* TCEP, pH 8.0) with dialysis. Protein was >98% pure by SDS-PAGE analysis, and was concentrated with Amicon Ultra YM10 membrane (Millipore, Bedford, MA) to micromolar concentrations. Purified cysteine mutants were stored at −80°C or conjugated to fluorophore as described below.

Each 11F8 cysteine variant (15–100 μM) was conjugated to fluorescein-5-maleimide (Molecular Probes, Eugene, OR). Fluorescein-5-maleimide was dissolved (50 mg/mL) in DMSO and 50× molar excess was added to a stirring solution of concentrated folded protein in conjugation buffer. The reaction proceeded at room temperature for 2 h with stirring and then 4°C for an additional 18 h. Free dye was removed with a P-10 column, 2.5 mL bed volume (Amersham, Piscataway, NJ) that had been equilibrated in conjugation buffer. Protein was dialyzed against 4 L of conjugation buffer for 24 h. The degree of labeling was calculated for each 11F8 variant by comparing the protein absorbance at 280 nm (extinction coefficient of 11F8 is 51,970 $cm^{-1}\ M^{-1}$)[33] with absorbance at 495 nm (extinction coefficient of fluorescein 83,000 $cm^{-1}\ M^{-1}$),[34] and correcting for the UV absorbance contributed by fluorescein at 280 nm. The labeling efficiencies for 11F8 variants ranged from 60 to 90%. Site-specificity of labeling was confirmed with wild-type 11F8 control labeling reactions, which showed no dye conjugation.

Synthesis, Purification, and Labeling of 1 Variants

Tetramethylrhodamine labeled ^{C12}**1** variant was synthesized containing a single copy of the modified base Amino-Modifier C6 dC (Glen Research, Sterling, VA) using standard phosphor-amidite chemistry. ^{C12}**1** was purified to >95% by HPLC as previously described.[17] Prior to conjugation, DNA was ethanol precipitated to remove reactive buffer salts. Each modified oligonucleotide was alkylated with 5-carboxytetramethylrhodamine succinimidyl ester (5-TAMRA SE, Molecular Probes, Eugene, OR). Briefly, 100 μg of a 25 mg/mL stock of each oligonucleotide in H_2O was alkylated with 200 μg of 5-TAMRA dissolved in 14 μL DMSO in 0.1*M* sodium tetraborate, pH 8.5, labeling buffer with a total reaction volume of 100 μL. The reaction proceeded at room temperature with stirring for 8 h. Each reaction mixture was precipitated twice with EtOH, and labeled oligonucleotides were purified by reverse-phase HPLC using a Platinum EPS C_8 column (Alltech, Deerfield, IL) equilibrated at 95% 0.1*M* triethylammonium acetate, pH 6.6, and acetonitrile. DNA was eluted with a linear gradient from 5 to 65% acetonitrile over 30 min. Subsequent analytical reverse-phase analysis showed that each TAMRA-labeled oligonucleotide was >95% pure. Each oligonucleotide was equilibrated with 4*M* NaCl for 12 h to ensure that all backbone counterions were Na^{2+} and sequences were desalted with a 2.5 mL bed volume PD-10 column (Amersham, Piscataway, NJ).

Equilibrium Fluorescence Affinity Measurement

Fluorescence measurements were carried out on a Spectronic AB2 fluorometer equipped with a magnetic stirrer and a thermostated cell block.[35] Briefly, 11F8 was diluted into titration buffer (20 m*M* Tris, 150 m*M* NaCl, pH 8.0) and equilibrated at 25°C. The intrinsic protein fluorescence (λ_{ex} 280 nm; 4 nm bandpass, λ_{em} 336 nm; 16 nm bandpass) was measured as a function of added DNA. No correction for the inner filter effect was necessary due to nonprohibitive absorbance of DNA. Analysis of the binding isotherms has been described elsewhere.[35]

Equilibrium Fluorescence Anisotropy Measurements

The fluorescence anisotropy of each of the six fluorescein labeled 11F8 mutants and tetramethylrhodamine labeled ^{C12R}**1** was determined first as a single species, then in complex with unlabeled **1** and 11F8, respectively, and finally in complex with ^{C12R}**1** and each ^{F}11F8 mutant, respectively. Excitation and emission bandpass filters were utilized to observe the anisotropies of fluorescein (ex. 480 ± 10 nm; em. 530 ± 10 nm; Andover Corporation, Salem, NH) and tetramethylrhodamine (ex. 560 ± 10 nm; em. 590 ± 10 nm) in isolation. Titration of ^{F}11F8 and ^{C12R}**1** with >10-fold excess of labeled DNA and protein, respectively, resulted in the same anisotropies as observed with 1 : 1 molar equivalents so that experiments were completed with equimolar amounts of 11F8 and **1**. The anisotropy of each complex (20 n*M* 11F8 or mutant and 20 n*M* **1** or variant) was measured, after equilibrating at room temperature for 5 min, as an average of 25 scans using a Beacon 2000 Fluorescence Polarization System (Invitrogen, Carlsbad, CA). Fluorescein and tetramethylrhodamine anisotropies for all ^{F}11F8•**1**, 11F8•^{C12R}**1**, and ^{F}11F8•^{C12R}**1** complexes were ≤0.20 validating the assumption of free fluorophore rotation upon complex formation as basis for using Förster theory in our stopped-flow FRET energy transfer analysis.[36]

Stopped-Flow FRET

Stopped-flow FRET experiments were conducted using a π*-CDF stopped-flow spectrophotometer from Applied Photophysics (Surrey, UK). The sample-handling unit was fitted with 2 mL syringes to give a mixing ratio of 1 : 1 v/v. In all cases, the fluorescein donor was excited with a Hg/Xe lamp at 436 nm (for optimal lamp intensity) using a 1.5 nm slit width, and 1000 data points were collected for each measurement over 5 s. The time-dependent change in FRET (tetramethylrhodamine fluorescence) was monitored using a 570 nm cutoff filter to eliminate any contribution from direct fluorescein excitation. Background correction was completed for each trace to remove any contribution from direct tetramethylrhodamine excitation. All measurements were made in 20 m*M* Tris-HCl, pH 8.0, 150 m*M* NaCl, 20% w/v sucrose at 5°C, and at least eight independent measurements were analyzed both individually and as an average by single or double exponential curve fitting algorithms. In experiments to determine the association rates for complex formation, [11F8] = 200 n*M* (prior to mixing) while the DNA was maintained in at least 10-fold excess [2, 2.5, 3.0, and 3.5 μM] to approximate pseudo-first-order reaction conditions. The second-order rate constant k_2 was calculated form the slope of k_{app} versus [DNA].

RESULTS

Selection of Fluorescent Probe Locations

To enable the FRET studies, sites for fluorescent probe attachment were determined for both 11F8 and **1** that did not perturb final complex formation. Antigen recognition primarily occurs through residues located in the six CDRs of the heavy and light chain variable regions.[37] A cysteine was introduced

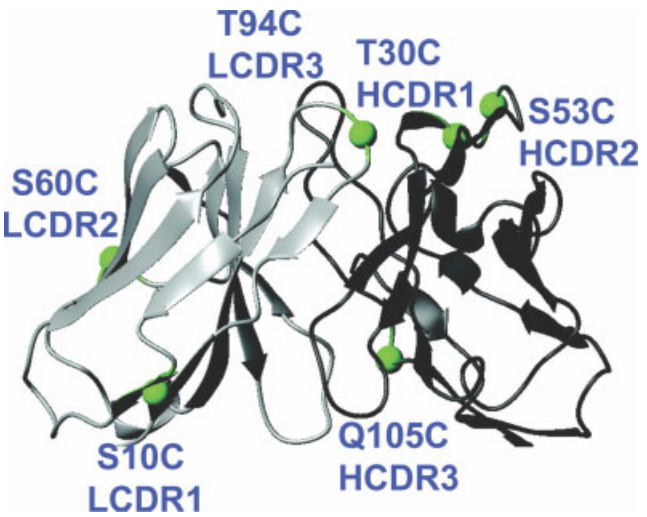

FIGURE 2 Schematic displaying the location of donor probes for stopped-flow FRET. The light chain variable region is shown in light gray and the variable heavy chain is shown in dark gray. Site-specific fluorescein attachment sites are labeled as green spheres.

via site directed mutagenesis either directly into or as close as possible to each of the six CDRs. Residues were selected for cysteine mutation based on a >50% relative solvent accessible surface area excluding residues that maintain canonical CDR structure or participate in CDR•CDR interactions to avoid introducing gross structural changes into the binding site.[38] On the basis of these criteria, cysteine mutations within HCDR1, HCDR2, and LCDR3 afforded reporters at $^{T30C}V_H$, $^{S53C}V_H$, and $^{T94C}V_L$ respectively. However, cysteine mutation to each loop residue in LCDR1, LCDR2, and HCDR3 rendered unstable protein or a mutant that did not bind **1**. Mutations to neighboring framework regions accessed cysteine mutants that did not perturb binding affinity. The closest HCDR3 reporter, $^{Q105C}V_H$, is three amino acids away from HCDR3, the closest LCDR1 reporter, $^{S10C}V_L$, is 13 amino acids away from LCDR1, and the closest LCDR2 reporter, $^{S60C}V_L$, is four amino acids away from LCDR2. The cytosine that forms the loop closing of base pair **1** (^{C12}**1**) was selected as the reporter of DNA conformation to afford six different donor•acceptor reporters for relative conformational changes between 11F8 and **1** during association (Figure 2).

When 11F8 and related mAbs bind DNA, a quench in tryptophan fluorescence is observed due to changes in the microenvironment of $^{W33}V_H$ in the binding pocket.[27] Binding affinity of the fluorescein and tetramethylrhodamine labeled variants was determined by monitoring the quench in trypotphan fluorescence upon complex formation. The affinity of the 11F8•**1** complex was not significantly affected by labeling in any of the six double-labeled complexes (Table I). In all cases, the fluorescein fluorescence was monitored and did not change throughout titration of ssDNA. Docking experiments suggest somatic mutation from serine to arginine at $^{31}V_H$ may result in more extensive conformational changes during recognition.[30] A second mutation from arginine to serine was introduced at $^{31}V_H$ in each of the six 11F8 loop reporters to determine the dynamics of the ^{R31S}11F8•**1** complex. Binding affinity of double mutants was not determined because it has been established that the $^{R31S}V_H$ mutation decreases affinity, and the objective of these experiments was to monitor the structural effects of reversion mutation.[29] However, previous studies suggest that little cooperativity exists between residues of 11F8.[29] Thus, we do not anticipate that cooperativity between any of these double mutants contribute to binding affinity.[29,39]

Stopped-Flow Fluorescence Resonance Energy Transfer

The quench in tryptophan fluorescence upon 11F8•**1** association has also been utilized to determine the rate constants for complex formation by stopped-flow.[27] Recognition of **1** by 11F8 proceeds in two steps: formation of an encounter complex, followed by a slow rate-limiting step that results in the high-affinity complex observed at equilibrium as shown in Scheme 1.[27] Kinetic parameters for related mAbs revealed that in the absence of a basic residue at $^{31}V_H$, recognition of **1** results in a single decrease in tryptophan fluorescence. The rates of the single step are slow and independent of [**1**] and thus correspond to rate limited formation of the high affinity complex (k_2) in 11F8•**1** recognition. These findings suggest that the loss of electrostatic contacts from a basic side chain coupled with the loss of a salt bridge to orient the ensuing

Table I Binding Affinity for ^{F}11F8 and ^{R}1

	11F8 K_d (nM)	HCDR1 K_d (rel K_d)	HCDR2 K_d (rel K_d)	HCDR3 K_d (rel K_d)	LCDR1 K_d (rel K_d)	LCDR2 K_d (rel K_d)	LCDR3 K_d (rel K_d)
1	1.6 ± 0.4	2.2 ± 1.4 (1.5)	0.7 ± 0.4 (0.5)	2.5 ± 0.8 (1.6)	1.3 ± 0.6 (0.9)	1.5 ± 0.4 (0.9)	0.9 ± 0.3 (0.6)
^{C12}**1**	4.2 ± 0.7 (2.6)	4.4 ± 0.5 (2.8)	1.8 ± 0.1 (1.1)	4.1 ± 1.4 (2.6)	4.2 ± 1.0 (2.6)	4.3 ± 0.5 (2.7)	3.7 ± 0.6 (2.3)

Binding affinity was measured in 20 mM Tris, 150 mM NaCl, pH 8.0 at 25 °C. Relative K_d values are normalized against the K_d for the wild-type 11F8•**1** complex and are listed in parentheses. Errors in K_d are standard deviations derived from a minimum of three independent assays.

$$11F8 + \mathbf{1} \underset{k_{-1}}{\overset{k_1}{\rightleftharpoons}} [11F8{\cdot}\mathbf{1}]^* \underset{k_{-2}}{\overset{k_2}{\rightleftharpoons}} 11F8{\cdot}\mathbf{1}$$

SCHEME 1

complex results in an altered association and likely conformation of the encounter complex. We used FRET to determine if conformational changes at the interface were mediated by $^{31}V_H$. Because individual steps in the 11F8 reaction pathway have discernable rates, we hypothesized that concerted structural changes accompanying complex formation could be resolved to specific steps based upon rate constants.

Our approach was to combine FRET and pre-steady-state kinetics to monitor the energy transfer of six different donor•acceptor pairs. Stopped-flow FRET cannot distinguish a priori between contributions to energy transfer resulting from inter-fluorophore distance changes with respect to more subtle fluorophore changes that are sensitive to binding events, but not related to biopolymer dynamics. Control experiments were completed to rule out a significant contribution to energy transfer by process such as change in fluorophore mobility or hydrophobicity of the solvent environment. Briefly, fluorescein and tetramethylrhodamine anisotropies for all ^{F}11F8•**1**, 11F8•^{C12R}**1**, and ^{F}11F8•^{C12R}**1** complexes were $\leq$0.20, validating the use of Förster theory for energy transfer studies (Table II). Additionally, background fluorescence of the donor only ^{F}11F8•**1** and acceptor only 11F8•^{C12R}**1** were subtracted from the FRET of each double-labeled ^{F}11F8•^{C12R}**1** complex, where ^{F}11F8 and ^{C12R}**1** describe fluorescein labeled and tetramethylrhodamine labeled variants, respectively. Tetramethylrhodamine fluorescence resulting from energy transfer for each ^{F}11F8•^{C12R}**1** complex was fit with either single or double exponential curve fitting algorithms.

Similar to the quench in tryptophan fluorescence upon 11F8•**1** association, the increase in tetramethylrhodamine fluorescence during ^{F}11F8•^{R}**1** recognition is biphasic (Figure 3). Although FRET association rates do not directly correspond with those obtained via tryptophan fluorescence, similar trends exist (Table III).[27] The initial fast increase in tetramethylrhodamine fluorescence is followed by a second slower increase in fluorescence. For five of the six complexes, k_1 was significantly faster than k_2. One complex ^{HCDR3F}11F8•^{C12R}**1** resulted in only a single exponential tetramethylrhodamine response that was independent of [**1**]. In all cases the rate of the initial phase (k_1) varied linearly with [**1**] typical of a bimolecular association process, and the rate of the second phase (k_2) was independent of [**1**]. As suggested previously for 11F8, it is likely that k_2 represents the formation of the high affinity complex.[27] Because FRET during association can be broken down into the two steps used to characterize 11F8•**1** association, amplitudes of each step describe the qualitative conformational changes throughout complex formation.

Stopped-flow FRET measures relative distance changes between two points rather than absolute distances, and describes the concerted movement of both an 11F8 CDR and **1** with respect to each other. Since energy transfer is distance dependent, fluorescein donor and tetramethylrhodamine acceptor fluorophores must be within $\sim$80 Å for energy transfer. Therefore, stopped-flow FRET cannot fully describe the association process because a portion of k_1 could occur before the detection limit of the method is achieved for particular donor–acceptor pairs. Direct comparison of k_1 is therefore impossible to evaluate, since the extent to which k_1 is observed is unknown. Alternatively, rate constants for the slow phase, k_2, were measured with good agreement between all of the six donor–acceptor pairs (1.1 $\pm$ 0.05 s^{-1}). FRET amplitudes indicate conformational change in the second step and lend further support that k_2 describes conforma-

Table II Fluorescence Anisotropies of Fluorescein and Tetramethylrhodamine Probes Determined Individually for Each Fluorophore and Complex

Anisotropy Conditions	11F8	HCDR1	HCDR2	HCDR3	LCDR1	LCDR2	LCDR3
1	NA	.10 $\pm$ .001	.11 $\pm$ .001	.08 $\pm$ .001	.10 $\pm$ .006	.10 $\pm$ .005	.07 $\pm$ .002
Donor alone, Fluorescein ^{C12R}**1**	.16 $\pm$ .002	NA	NA	NA	NA	NA	NA
Acceptor alone, Rhodamine ^{F}11F8•^{C12R}**1**	NA	.11 $\pm$ .004	.12 $\pm$ .001	.07 $\pm$ .004	.10 $\pm$ .002	.11 $\pm$ .003	.05 $\pm$ .005
Double labeled, Fluorescein ^{F}11F8•^{C12R}**1**	NA	.20 $\pm$ .001	.19 $\pm$ .001	.15 $\pm$ .001	.20 $\pm$ .002	.20 $\pm$ .002	.15 $\pm$ .001
Double labeled, Rhodamine							

Errors are the standard deviations for a minimum of three independent assays.

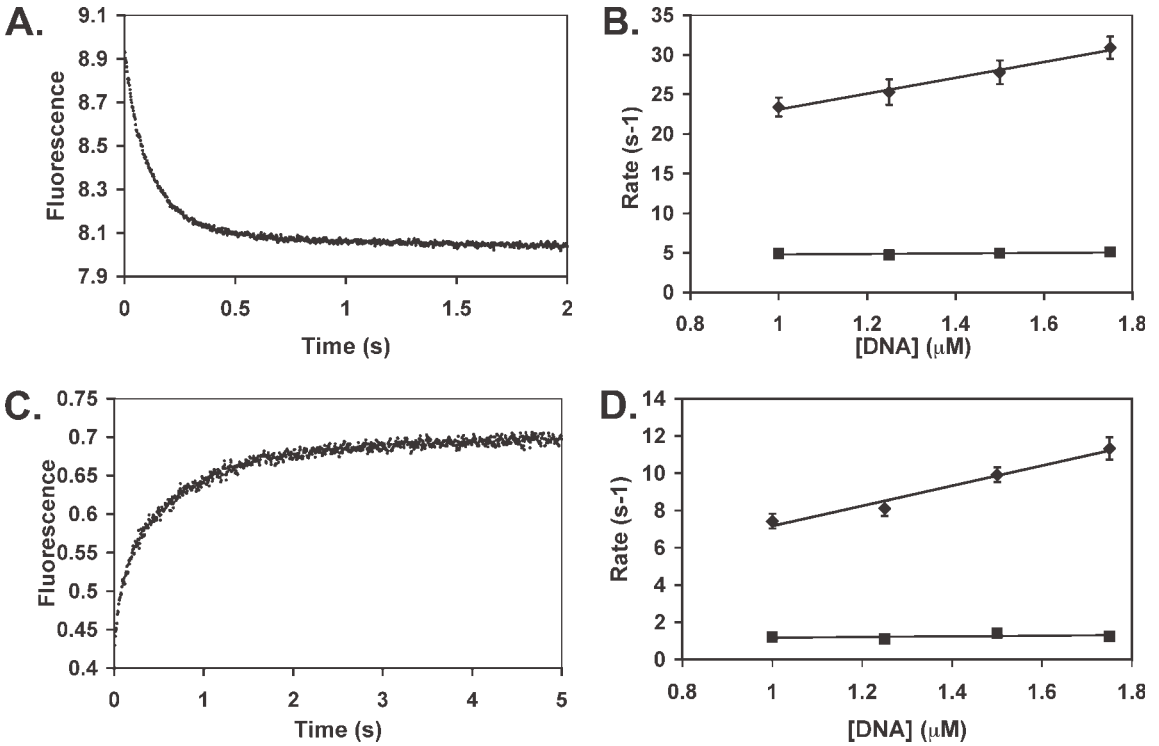

FIGURE 3 Stopped-flow fluorescence data for the interaction between 11F8 and **1**. (A) Association trace for the interaction between 11F8 (200 n*M*) and **1** (2 μM). The excitation wavelength was set at 280 nm to monitor the decrease in tryptophan fluorescence. The initial fast change in fluorescence has a rate of 23.4 $\pm$ 2.1 s^{-1}, whereas the rate of the second slow signal change is 4.9 $\pm$ 0.4 s^{-1}. (B) Linear dependence of the initial rate (k_{app}) on [**1**]. The second order rate constant (k_1) describing the fast step (◆) was calculated to be 9.4 $\pm$ 0.8 s^{-1} in 20% sucrose from the slope of the plot. The second slower rate (■) was shown to be independent of [**1**] under pseudo-first-order conditions. (C) Representative FRET association trace for the interaction between ^{LCDR1F}11F8 (200 n*M*) and ^{C12R}**1** (2 μM). The excitation wavelength was set at 436 nm and rhodamine fluorescence resulting from FRET was measured above 570 nm. The initial fast change in fluorescence has a rate of 9.1 $\pm$ 0.6 s^{-1}, whereas the rate of the second slow signal change is 1.1 $\pm$ 0.1 s^{-1}. (D) Linear dependence of the rates (k_{app}) on. [**1**] The second order rate constant (k_1) describing the fast step (◆) was calculated to be 3.9 $\pm$ 0.3 s^{-1} in 20% sucrose from the slope of the plot. The second slower observed rate (■) was independent of [**1**] over the concentration range tested.

tional adjustments during the progression from encounter complex to high affinity complex as hypothesized. The rates and amplitudes for k_2 were compared to evaluate the relative dynamics between 11F8 CDRs and **1** (Table III). It is interesting to note that ^{HCDR1F}11F8●^{C12R}**1**, ^{LCDR1F}11F8●^{C12R}**1**, and ^{LCDR2F}11F8●^{C12R}**1** undergo greater conformational change during complex formation than the other three CDRs and **1** (Figure 4).

When a single somatic mutation is reverted to germline ($^{R31S}V_H$), 11F8 loses sequence-specificity, and the thermodynamic and kinetic parameters for ssDNA recognition resemble the clonally related, nonsequence-specific, nonpathogenic mAbs 9F11 and 15B10.[28] Both 9F11 and 15B10 have a serine side chain at $^{31}V_H$. To investigate the dynamics of the CDRs during complex formation in the absence of arginine, six corresponding ^{R31SF}11F8●^{C12R}**1** complexes bearing mutation to serine and conjugated to fluorescein were monitored by stopped-flow FRET (Table IV). A single exponential fluorescence response was expected based upon previous observations that removal of a basic side chain at $^{31}V_H$ resulted in a single exponential quench in tryptophan fluorescence.[26] When observed, the change in tetramethylrhodamine fluorescence for the double mutants fit a single exponential with a rate independent of [**1**]. Rates for k_2 were similar to those observed with arginine instead of serine at $^{31}V_H$. These data provide further support that a rate-limiting conformational change is observed both in the presence and absence of arginine.

Because FRET efficiency directly correlates to distance, changes in FRET efficiency (indicated by an increase or decre-

Table III Rate Constants and FRET Amplitudes Measured During ^{F}11F8•^{R}1 Association

Complex	k_1 ($\mu M^{-1}s^{-1}$)	k_2 (s^{-1})	Amp k_1 (Fluorescence Units)	Amp k_2 (Fluorescence Units)
^{HCDR1F}11F8•^{C12R}**1**	8.6 ± 1.0	1.1 ± 0.1	0.13 ± .02	0.29 ± .01
^{HCDR2F}11F8•^{C12R}**1**	8.4 ± 0.8	1.1 ± 0.1	0.07 ± .04	0.10 ± .01
^{HCDR3F}11F8•^{C12R}**1**	NO	1.0 ± 0.1	NO	0.06 ± .01
^{LCDR1F}11F8•^{C12R}**1**	3.9 ± 0.3	1.1 ± 0.1	0.12 ± .01	0.26 ± .01
^{LCDR2F}11F8•^{C12R}**1**	9.8 ± 1.0	1.1 ± 0.1	0.14 ± .03	0.26 ± .01
^{LCDR3F}11F8•^{C12R}**1**	1.6 ± 0.2	1.0 ± 0.3	0.02 ± .01	0.03 ± .01

Rate constants were measured in 20 mM Tris, 100 mM NaCl, pH 8.0, 20% w/v sucrose at 5 °C. ^{HCDR3F}11F8•^{C12R}**1** association occurs in one step. The observed rate is independent of [**1**] and is related to the formation of the high affinity complex (k_2) in 11F8•**1** association, which is also independent of [**1**]. The single association rate for ^{HCDR3R}11F8•^{C12R}**1** is therefore reported as k_2 for comparison. NO stands for not observed. Errors are standard deviations derived from a minimum of eight traces.

ase in tetramethylrhodamine fluorescence as a result of energy transfer) are related to the magnitude of conformational change that occurs upon binding. While k_2 for the serine double mutants is similar, amplitudes are significantly smaller and often in the opposite direction (decreases in tetramethylrhodamine fluorescence are observed in ^{R31S}11F8•**1** instead of increases as observed in 11F8•**1**) (Table IV). These data suggest that in the absence of arginine at $^{31}V_H$, donor and acceptor fluorophores move slightly further apart as the encounter complex reaches equilibrium. In two cases (^{R31SHCDR1F}11F8•^{C12R}**1** and ^{R31SLCDR2F}11F8•^{C12R}**1**) there was no change in tetramethylrhodamine fluorescence observed. This donor and acceptor exhibit energy transfer at equilibrium (transfer efficiency of 0.67 ± 0.1 and 0.48 ± 0.2, respectively) and so the absence of a change in transfer efficiency cannot be attributed to a lack of FRET, but rather lack of a detectable conformational change. Collectively, these data suggest that without arginine at $^{31}V_H$, there is less structural rearrangement at the binding site.

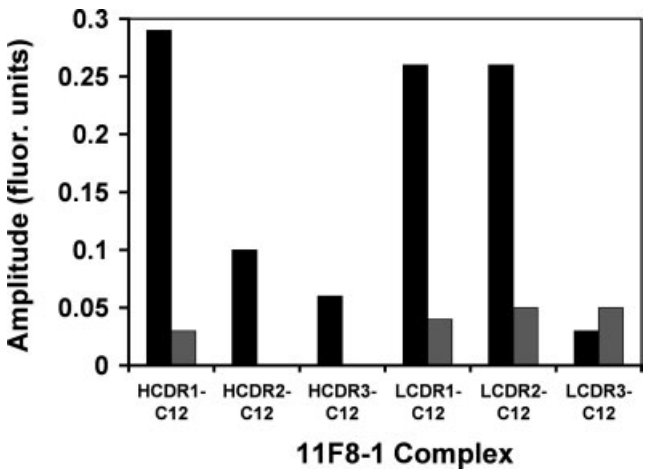

FIGURE 4 Change in FRET amplitude during k_2 for the six ^{F}11F8•^{C12R}**1** complexes in the presence (black) and absence (gray) of binding site arginine at $^{31}V_H$. The CDR location of fluorescein is described by HCDR1, HCDR2, HCDR3, LCDR1, LCDR2, and LCDR3 while the rhodamine probe is located on C12 (^{C12}**1**).

DISCUSSION

There are only a few high-resolution structures of anti-nucleic acid autoantibodies and their respective mAb•antigen complexes: DNA-1•dT$_{3/5}$,[7,31] BV04-01•d(pT),[5] and Jel 103•rI.[40] These three anti-ssDNA/RNA mAbs help describe the components of nucleic acid recognition, and provide insight towards antibody flexibility during binding. In particular, large structural differences between DNA-1 in complex with either oligo thymine or HEPES salt suggests that conformational flexibility accounts for specificity while a somatic

Table IV Rate Constant and FRET Amplitudes Measured During ^{R31SF}11F8•^{R}1 Association

Complex	k_2 (s^{-1})	Amp k_2 (Fluorescence Units)
^{HCDR1F}11F8•^{C12R}**1**	2.5 ± 1.0	0.03 ± .01
^{HCDR2F}11F8•^{C12R}**1**	–	–
^{HCDR3F}11F8•^{C12R}**1**	–	–
^{LCDR1F}11F8•^{C12R}**1**	0.2 ± 0.1	0.04 ± .01
^{LCDR2F}11F8•^{C12R}**1**	1.1 ± 0.1	0.05 ± .01
^{LCDR3F}11F8•^{C12R}**1**	1.3 ± 0.3	0.05 ± .01

Rate constants were measured in 20 mM Tris, 100 mM NaCl, pH 8.0, 20% w/v sucrose at 5 °C. (–) indicate complexes where no change in energy transfer is observed. When a change in energy transfer is observed, it always fits a single exponential. Since the observed rate is independent of [**1**] it is related to the formation of the high affinity complex (k_2) in 11F8•**1** association, which is also independent of [**1**]. The single association rate is therefore reported as k_2 for comparison. Decreases (shown in italic) in rhodamine fluorescence are observed. Errors are standard deviations derived from a minimum of eight traces.

mutation helps to lock certain ligands into an optimal binding site.[7] Consistent with our observations of increased conformational change following somatic mutation, Schuermann et al. suggest that structural plasticity could provide a mechanism by which anti-DNA antibodies can access binding sites for diverse host ligands, and thereby contribute to pathogenicity.[7]

The body of work describing the binding properties of 9F11, and 15B10 suggests that similar to BV04-01, DNA-1, and Jel 103, these mAbs utilize $^{Y32}V_L$, a hydrogen bonding residue at $^{91}V_L$, and an aromatic side-chain at the tip of HCDR3 to bind ssDNA.[28,30] Crystal structures of BV04-01, DNA-1, and Jel 103 complexes reveal a nucleotide sandwiched between two aromatic residues in the binding pocket. Interestingly, both BV04-01 and DNA-1 use two binding site residues to flank a single thymine nucleotide (although multiple thymine residues are available), and Jel 103 stacks with a single nucleotide as well (although the Jel 103 crystal was soaked with rI nucleotides). Similar to 9F11 and 15B10, both DNA-1, and Jel103 have a serine at $^{31}V_H$ whereas BV04-01 has a threonine. A model of the ^{R31S}11F8●**1** complex (structurally similar to 9F11 and 15B10) suggests that $^{Y32}V_L$, $^{H91}V_L$, and $^{Y100}V_H$ at the tip of HCDR3 interact with **1**.[30] It is likely that 9F11 and 15B10 recognition of ssDNA occurs through the common structural hot spot observed in the BV04-01, DNA-1, and Jel 103 complexes.

While other ssDNA binding proteins differ from anti-DNA autoantibodies in the secondary structural motifs that interact with DNA, they often utilize both surface complementarity and conformational change. For example, *Oxytricha nova* telomere end binding protein (*On*TEBP) binds ssDNA with high affinity (nM-pM) and sequence-specificity through extensive surface complementarity and conformational change.[41,42] Structural comparisons of both cognate and noncognate *On*TEBP●ssDNA complexes revealed extensive binding site reorganization to accommodate cognate vs. noncognate nucleic acid sequences.[43] Additionally, the TraI protein is similar to the variable heavy chain of 11F8 and clonally related mAbs 9F11 and 15B10 in that despite high sequence homology in related TraI domains (for recognition of F or R100 plasmid DNA), sequence variability at only two positions entirely mediates unique specificities. Two different TraI domains containing either R193/Q201 (F) or Q193/R201 (R100) discriminate between binding sites that differ by two of eleven nucleotides.[44] Mutating these two side chains located on opposite sides of the binding site (R193Q/Q201R in F or Q193R/R201Q in R100) confers specificity for the noncognate site over the cognate site in both cases.[45]

Somatically mutated $^{R31}V_H$ is located at the periphery of the 11F8 binding pocket and several lines of evidence suggest that it forms a salt bridge with the ssDNA backbone.[26,28–30] Together with conserved $^{R98}V_H$, $^{R31}V_H$ likely facilitates dual salt bridge contacts to orient the ensuing sequence-specific 11F8●**1** complex. The 11F8●**1** and ^{R31S}11F8●**1** models suggest that conformation and contact changes facilitated by the $^{S31R}V_H$ somatic mutation results in recognition in part similar but also unique from other anti-ssDNA. We hypothesize that the $^{R31}V_H$ salt bridge with **1** affords sequence and register discrimination in the encounter complex. The 11F8●**1** model proposes interactions between $^{R31}V_H$ and **1** cause loss of interaction with $^{91}V_L$ and gain of direct contacts with side chains in V_H, not previously associated with ssDNA recognition ($^{W33}V_H$, $^{R96}V_H$, and $^{L97}V_H$), collectively shifting the binding site towards the heavy chain.[30]

A change in specific heat upon complex formation can be attributed to increased burial of hydrophobic surface area, and in some cases conformational change.[46] Because the model of the 11F8●**1** complex and the model of the ^{R31S}11F8●**1** complex suggest similar buried surface areas, differences in specific heat capacity upon ssDNA binding could be indicative of conformational change. Comparison of changes in specific heat capacity upon recognition of **1** versus a thymine-rich ligand (**T7**) by 11F8, 9F11, and 15B10 is consistent with conformational change during sequence-specific recognition of **1**.[46] When 11F8, 9F11, and 15B10 bind to **T7** there is no ΔC_P, even though a significant amount of hydrophobic surface area is occluded when aromatic side chains stack with thymine at the interface. 9F11 and 15B10 recognition of **1** occurs with no ΔC_P similar to recognition of **T7**. However, the ΔC_P for 11F8 binding to **1** is accompanied by $-\Delta C_P$ (-1.3 kcal mol^{-1} K^{-1}), which supports our FRET data suggesting greater conformational change during sequence-specific recognition of **1**.[35]

Collectively, structural modeling and FRET data propose that altered surface complementarity is achieved through $^{R31}V_H$ dependent conformational rearrangement during sequence-specific recognition of **1** by 11F8. The model of the 11F8●**1** complex together with mutagenesis data indicate a second thymine stacks between $^{Y100}V_H$ and $^{W33}V_H$, and that direct contacts exist between the guanidinium side chain and base edge hydrogen bond acceptors, both of which do not exist in the model of ^{R31S}11F8●**1**. These data imply that $^{R31}V_H$ affords 11F8 sequence-specificity in part by mediating conformational change, and together with sequence-specific contacts, may mediate the transition from nonpathogenic to pathogenic phenotype for a lupus autoantibody.

REFERENCES

1. Wilson, I. A.; Stanfield, R. L. Curr Opin Struct Biol 1993, 3, 113–118.

2. Dall'Aqua, W.; Goldman, E. R.; Lin, W.; Teng, C.; Tsuchiya, D.; Li, H.; Ysern, X.; Braden, B. C.; Li, Y.; Smith-Gill, S. J.; Mariuzza, R. A. Biochemistry 1998, 37, 7981–7991.
3. Mariuzza, R. A.; Phillips, S. E.; Poljak, R. J. Annu Rev Biophys Biophys Chem 1987, 16, 139–159.
4. Sundberg, E. J.; Mariuzza, R. A. Adv Protein Chem 2002, 61, 119–160.
5. Herron, J. N.; He, X. M.; Ballard, D. W.; Blier, P. R.; Pace, P. E.; Blothwell, A. L. M.; Voss, E. W. J.; Edmundson, A. B. Proteins 1991, 11, 159–175.
6. Pellequer, J.-L.; Chen, S. W. W.; Keum, Y. S.; Karu, A. E.; Li, Q. X.; Roberts, V. A. J Mol Recognit 2005, 18, 282–294.
7. Schuermann, J. P.; Prewitt, S. P.; Davies, C.; Deutscher, S. L.; Tanner, J. J. J Mol Biol 2005, 347, 965–978.
8. Parkkinen, T.; Nevanen, T. K.; Koivula, A.; Rouvinen, J. J Mol Biol 2006, 357, 471–480.
9. Midelfort, K. S.; Hernandez, H. H.; Lippow, S. M.; Tidor, B.; Drennan, C. L.; Wittrup, K. D. J Mol Biol 2004, 343, 685–701.
10. Valjakka, J.; Takkinenz, K.; Teerinen, T.; Soderlund, H.; Rouvinen, J. J Biol Chem 2002, 277, 4183–4190.
11. Monaco-Malbet, S.; Berthet-Colominas, C.; Novelli, A.; Battai, N.; Piga, N.; Cheynet, V.; Mallet, F.; Cusack, S. Structure 2000, 8, 1069–1077.
12. Bongini, L.; Fanelli, D.; Piazza, F.; Rios, P. D. L.; Sandin, S.; Skoglund, U. Biophys Chem 2005, 115, 235–240.
13. Puntheeranurak, T.; Wildling, L.; Gruber, H. J.; Kinne, R. K.; Hinterdorfer, P. J Cell Sci 2006, 119, 2960–2967.
14. Mallender, W. D.; Ferreira, S. T.; Voss, E. W. J.; Colelho-Sampaio, T. Biochemistry 1994, 33, 10100–10108.
15. Isenberg, D. A.; Ehrenstein, M. R.; Longhurst, C.; Kalsi, J. K. Arthritis Rheum 1994, 37, 169–180.
16. Ravirajan, C. T.; Rowse, L.; MacGowan, J. R.; Isenberg, D. A. Rheumatology 2001, 40, 1405–1412.
17. Swanson, P. C.; Ackroyd, P. C.; Glick, G. D. Biochemistry 1996, 35, 1624–1633.
18. Swanson, P. C.; Yung, R. L.; Blatt, N. B.; Eagen, M. A.; Norris, J. M.; Richardson, B. C.; Johnson, K. J.; Glick, G. D. J Clin Invest 1996, 97, 1748–1760.
19. Catasti, P.; Chen, X.; Mariappan, S. V.; Bradbury, E. M.; Gupta, G. Genetica 1999, 106, 15–36.
20. Lipes, B. D.; Keene, J. D. RNA 2002, 8, 762–771.
21. Sano, H.; Moritoto, C. J Immunol 1982, 128, 538–539.
22. Krapf, F. E.; Hermann, M.; Leitmann, W.; Kalden, J. R. Rheumatol Int 1989, 9, 115–121.
23. Sano, H.; Taki, O.; Harat, N.; Yoshinaga, K.; Kodama-Kamada, I.; Sasaki, T. Scand J Immunol 1989, 30, 51–63.
24. Terada, K.; Okuhara, E.; Kawarada, Y.; Hirose, S. Biochem Biophys Res Commun 1991, 174, 323–330.
25. Stevens, S. Y.; Glick, G. D. Biochemistry 1999, 38, 560–568.
26. Beckingham, J. A.; Cleary, J.; Bobeck, M.; Glick, G. D. Biochemistry 2003, 42, 4118–4126.
27. Beckingham, J. A.; Glick, G. D. Bioorg Med Chem 2001, 9, 2243–2252.
28. Bobeck, M. J.; Cleary, J.; Beckingham, J. A.; Ackroyd, P. C.; Glick, G. D. Accepted in Biopolymers, 2007-0005 DOI 10.1002/bip.20691, in this issue.
29. Cleary, J.; Glick, G. D. Biochemistry 2003, 42, 30–41.
30. Bobeck, M.; Rueda, D.; Walter, N. G.; Glick, G. D. Has been submitted to Biochemistry 1/29/07.
31. Tanner, J. J.; Komissarov, A. A.; Deutscher, S. L. J Mol Biol 2001, 314, 807–822.
32. Bendich, A. J.; Bolton, E. T. The DNA-Agar Procedure, 1968.
33. Mach, H.; Middaugh, C. R.; Lewis, R. V. Anal Biochem 1992, 200, 74–80.
34. Haugland, R. P. Handbook of Fluorescent Probes and Research Products; Molecular Probes: Eugene, OR, 2005.
35. Ackroyd, P. C.; Cleary, J.; Glick, G. D. Biochemistry 2001, 40, 2911–2922.
36. Haas, E.; Katchalski-Katzir, E.; Steinberg, I. Z. Biochemistry 1978, 17, 5064–5070.
37. Shlomchik, M. J.; Aucoin, A. H.; Pisetsky, D. S.; Weigert, M. G. Proc Natl Acad Sci USA 1987, 84, 9150–9154.
38. Chothia, C.; Lesk, A. M. J Mol Biol 1987, 196, 901–917.
39. Schreiber, G.; Fersht, A. R. J Mol Biol 1995, 248, 478–486.
40. Pokkuluri, R. P.; Bouthillier, F.; Li, Y.; Kuderova, A.; Lee, J. C.; Cygler, M. J Mol Biol 1994, 243, 283–297.
41. Mitton-Fry, R. M.; Anderson, E. A.; Theobald, D. L.; Glustrom, L. W.; Wuttke, D. S. J Mol Biol 2004, 338, 241–255.
42. Larkin, C.; Datta, S.; Harley, M. J.; Anderson, B. J.; Eblie, A.; Hargreaves, V.; Schildbach, J. F. Structure 2005, 13, 1533–1544.
43. Theobald, D. L.; Schultz, S. C. EMBO J 2003, 22, 4314–4324.
44. Harley, M. J.; Schildbach, J. F. Proc Natl Acad Sci USA 2003, 100, 11243–11248.
45. Stern, J. C.; Anderson, B. J.; Owens, T. J.; Schildbach, J. F. J Biol Chem 2004, 279, 29155–29159.
46. Record, M. T. J.; Lohman, T. M.; deHaseth, P. J Mol Biol 1976, 107, 145–158.

Reviewing Editor: Kenneth Breslauer